

Measuring PM_{2.5} concentrations from a single smartphone photograph

Shiqi YAO^{1,†}, Fei WANG^{1,†}, Bo HUANG^{1,2,3*}

¹Department of Geography and Resources Management, The Chinese University of Hong Kong, Hong Kong SAR

²Institute of Space and Earth Information Science, The Chinese University of Hong Kong, Hong Kong SAR

³Shenzhen Research Institute, The Chinese University of Hong Kong, Hong Kong SAR

*Correspondence to: bohuang@cuhk.edu.hk (Bo Huang)

Supplementary Information

Section S1 Details of the sky discoloration

1.1. Sky separation

Sky discoloration can essentially serve as an important indicator of impaired outdoor scenes caused by particulate matter. For example, on a clear day, Rayleigh scattering [1] dominates in the scattering process and is responsible for the blue color of the sky; on a dense hazy day, Mie scattering [2] is the dominant factor, resulting in a white sky. This phenomenon implies that the color of the sky might help characterize the loadings of airborne particulate matter.

Clearly, separating the sky from smartphone photographs is essential to quantify sky discoloration. For the purpose of separating the sky from photos, we take three dominant features of the sky: 1) the position of the sky is normally found at the top of the photo; 2) the texture gradients are limited in the sky regions; and 3) the color difference between a potential patch of sky and the reference color center should be as small as possible. According to these

three assumptions, we assume that the probability of sky patches P_{sky} is dependent on the three parameters and that it is given as follows:

$$P_{sky} = P_{pos} \times P_{\sigma I} \times P_{color} \quad (S1)$$

where $P_{pos} = \exp(-(n/H)^2)$ is the probability model for the position of the sky found from the upper part of the given image, wherein parameters n and H are the position of the current pixel and the height of the image, respectively. σI is the texture gradient in the horizontal and vertical directions. The last probability, P_{color} , is a three-dimensional Gaussian function that measures the deviation between the color component of the potential sky region and the reference color center intensities in the YUV color space. In this experiment, regions with P_{sky} exceeding 0.65 are regarded as sky regions.

1.2. Determination of empirical standard color value

Typically, to quantify the discoloration level of the sky in bad weather from a clear day, two or more photographs of the same scenes are required [3]. However, we are dealing with only a single photograph. Our solution is to determine an empirical standard color value of the separated sky regions from smartphone photographs. To obtain the empirical standard color value, we gathered 517 pictures captured under good weather, i.e., $PM_{2.5}$ concentrations less than $20 \mu g/m^3$, and transformed photographs from the RGB color space to the HSI color space. Then, the average color intensities of the sky region for each color channel were calculated independently. Fig. S1 demonstrates the sky result obtained using the sky probability model as well as the representation in the HSI color space.

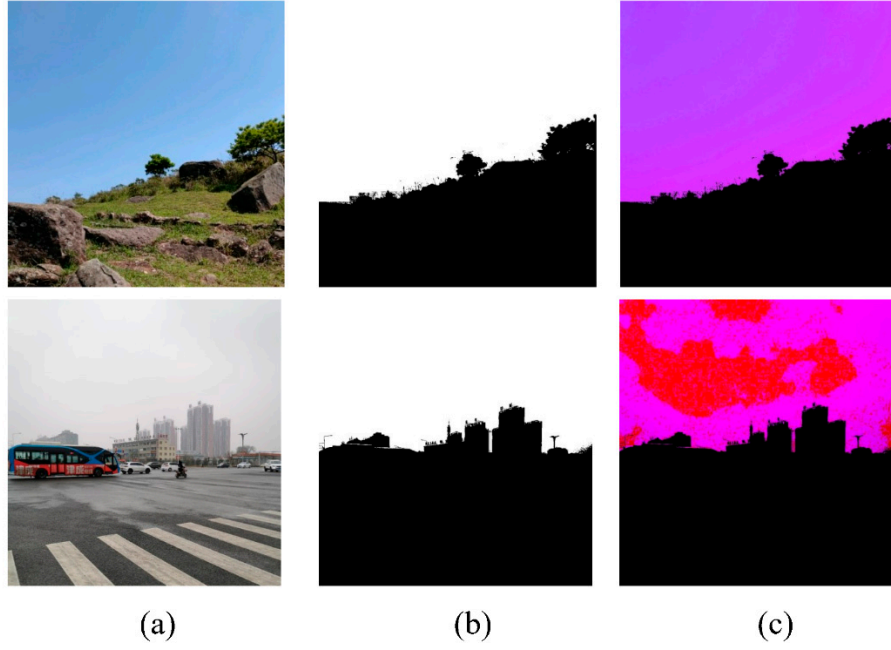


Figure. S1. Haze cues from the sky only. Starting from the input photograph (a), we extract the sky regions (b) with the sky probability model. The extracted sky regions in the HSI color space are presented in (c) under two distinct environmental conditions.

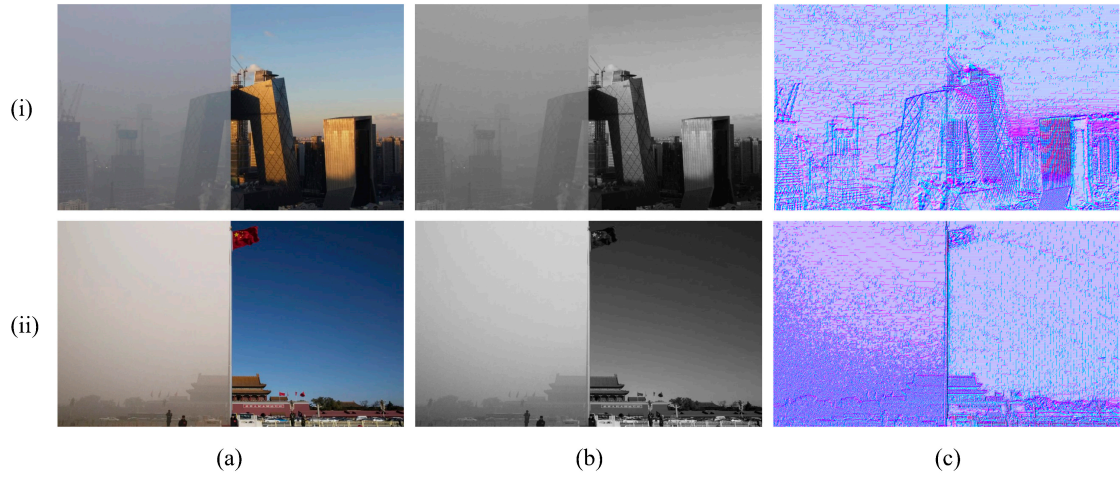


Figure. S2. Examples of photographs (a) transformed luminance maps (b), and luminance gradient maps (c) under two weather conditions, clear and heavy haze conditions, for photographs in which non-Lambertian regions dominate (i) and Lambertian regions dominate (ii).



Figure. S3. Examples of the direct sun-glint.

Section S2 Experiments on albedo

Albedo is a measure of reflectivity and associated with surface materials. To find out the range of albedo differences within one building, we conducted in-site measurements, quantified the albedo differences on two general types of buildings categorized by facades: glass façade, concrete façade. The albedo of each object is calculated as the ratio of solar radiation in and out. Therefore, we manually measured the in- and out- solar radiation using an instrument, namely Solarmeter [4]. Experiments in [5] proves that the albedo differences are nearly similar within one object at a given time. Basis on the evidence, we also collected more than 100 photographs, and each of them contains the sun-glint effects and measured the differences reflected on the photographs. Table S1 lists the experimental results. Last, we empirically found that the top 1% is an appropriate and relatively safe threshold for removing the sun glint effect. It should be noted that this threshold for removing the sun glint effect is suitable only for smartphone photographs in this study.

Table S1

The measured albedo in two general types of buildings.

Material of building surface	Albedo in Glint regions	Non-glint regions	Albedo differences
Glass façade	0.3871	0.1806	0.2065
Concrete façade	0.2561	0.0671	0.189

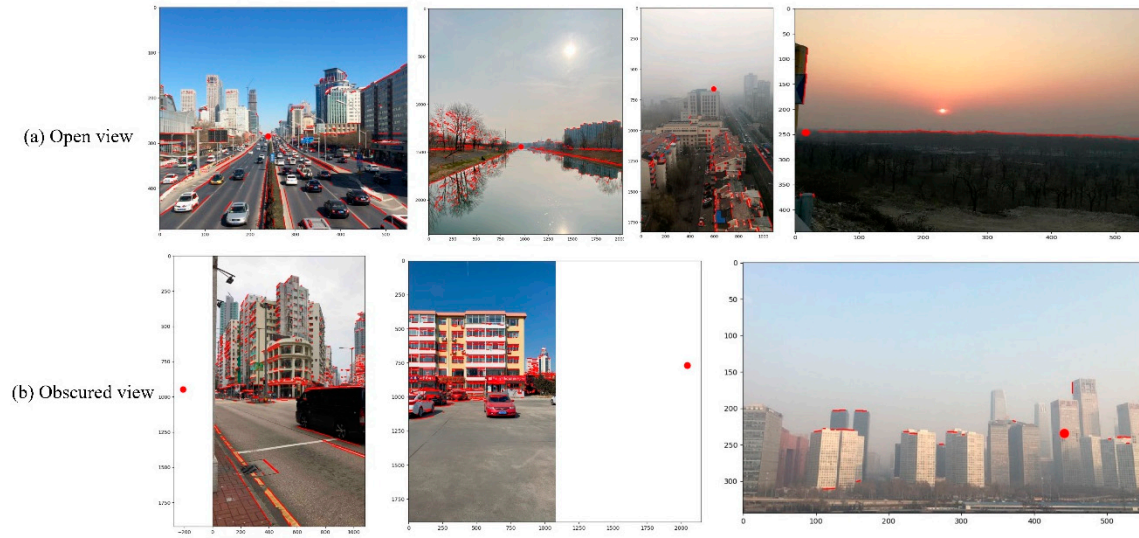


Figure. S4. Detected vanishing points (red dots) in (a) open view photographs and (b) obscured view photographs.

Table S2. Specifications of the Nature Clean sensor

Model	PAM1501
Dimension $W \times H \times D$ (mm)	$71 \times 55 \times 14.3$
Detectable PM	2.5, 10 μm
Measurement Technology	Laser scattering
Operation electricity	< 100 mA
Operation temperature	-10 to 50 $^{\circ}C$
Operation humidity	0 to 95%
Measurement accuracy	99% $\geq 2.5 \mu m$, 99% $\geq 10 \mu m$



Figure S5. Successful (a) and failed (b) example photographs with their observed and estimated $\text{PM}_{2.5}$ concentrations.

	Outdoor man-made				Outdoor natural		
C1 Transportations (roads, parking, airports, etc.)				C4 Water			
C2 Sports fields, parks, leisure's spaces				C5 Mountain, hills			
C3 Buildings, commercial buildings, markets				C6 Man-made elements			

Figure. S6. Examples photographs in each outdoor scene category.

Table S3. Detailed description of each sub-category.

1 st -level scene hierarchy	Outdoor man-made			Outdoor natural		
	Category index	Descriptions	*Counts	Category index	Descriptions	*Counts
2 nd -level scene hierarchy	C1	Transportations (roads, parking, airports, etc.)	314	C4	Water	502
	C2	Sports fields, leisure spaces	915	C5	Mountains, hills	107
	C3	Buildings, commercial building shops, markets	849	C6	Man-made elements	258

*Counts: the number of collected photographs in a specific category.

References

1. Rayleigh, Lord XXXIV. On the Transmission of Light through an Atmosphere Containing Small Particles in Suspension, and on the Origin of the Blue of the Sky. *The London, Edinburgh, and Dublin Philosophical Magazine and Journal of Science* **1899**, 47, 375–384, doi:10.1080/14786449908621276.
2. Middleton, W.E.K. Vision through the Atmosphere. In *Geophysik II / Geophysics II*; Bartels, J., Ed.; Handbuch der Physik / Encyclopedia of Physics; Springer: Berlin, Heidelberg, 1957; pp. 254–287 ISBN 978-3-642-45881-1.
3. Liu, X.; Song, Z.; Ngai, E.; Ma, J.; Wang, W. PM2.5 Monitoring Using Images from Smartphones in Participatory Sensing. In Proceedings of the 2015 IEEE Conference on Computer Communications Workshops (INFOCOM WKSHPS); IEEE: Hong Kong, Hong Kong, April 2015; pp. 630–635.
4. Solar light company Solarmeter Available online: <https://www.solarmeter.com/> (accessed on 18 November 2021).
5. Lalonde, J.-F.; Efros, A.; Narasimhan, S. *Estimating Natural Illumination from a Single Outdoor Image*; 2009; p. 190;.